

# Islanding and Dynamic Reconfiguration for Resilience Enhancement of Active Distribution Systems

Jianchun Xu, Tingting Zhang, Yaxin Du, Wen Zhang\*  
School of Electrical Engineering, Shandong University  
Jinan, China  
[zhangwen@sdu.edu.cn](mailto:zhangwen@sdu.edu.cn)

Tianyou Yang, Jifu Qiu  
State Grid Qingdao Power Supply Co. Ltd.  
Qingdao, China

**Abstract**—Increasingly frequent extreme weather events cause power outages in active distribution systems. Islanding and fault reconfiguration are effective approaches to service restoration and resilience enhancement. This paper proposes a multi-stage switch strategy based on dynamic programming (DP), considering both islanding and fault reconfiguration. First, numerous expected fault scenarios are constructed based on meteorological forecast and vulnerability analysis of system components, from which typical ones are selected by their information entropy. Second, for each typical scenario, a multi-stage switch strategy considering both islanding and fault reconfiguration is developed through DP. The objective is to make a tradeoff between minimizing total power shortage and minimizing the number of switching operations over the whole event's duration. The constraints comprise power flow limits, nodal voltage limits, and distributed generators' capabilities. Finally, a risk-based resilience assessment is performed and the resilience improvement is presented. Tests on the IEEE 33-bus distribution system demonstrate the effectiveness of the proposed method.

**Index Terms**—Active distribution systems; dynamic programming; islanding; reconfiguration; resilience enhancement.

## I. INTRODUCTION

Considering the global climate changes in recent years, increasingly frequent extreme weather disasters occur worldwide. It will result in large-scale power outages and bring serious economic losses and social impact [1-4]. Located at the end of power systems, distribution systems are the key to directly supply power to customers. Therefore, it is important to keep distribution systems under normal operation when exposed to extreme weather. In this condition, the resilience of distribution systems is introduced to reflect their ability to resist extreme weather disasters, to reduce fault losses, and to restore to the original state as soon as possible after the fault occurs [5,6]. In recent years, the researches on resilience have received more and more attention [7-12].

The basic prerequisite for resilience enhancement is the resilience analysis of distribution systems. According to the definition of resilience, a distribution system will go through three stages when an extreme weather event occurs: before, during, and after the fault [7, 8]. In order to improve the resilience of distribution systems, it is necessary to implement a strategy to restore loads from faults. By this means, more power can be supplied to the users, especially the critical loads. Based on different typhoon strengths and load levels, reference [9] studied the effectiveness of line reinforcement components, double-circuit construction, and shortening of fault repair time on the resilience enhancement of distribution systems. The influence of hardening the distribution lines on the distribution systems resilience was investigated in [10]. At present, the researches on the resilience improvement measures of distribution systems mainly focus on the strategy of overhead line cable and replacement of more hardening lines. However, the investment for infrastructure hardening is so high that limits its application to large-scale distribution systems. With the integration of distributed generators (DGs), the loads can be powered by the DGs to enhance the resilience of distribution systems [11]. However, merely partial loads can be restored by DGs alone due to the capacity limitation of DGs. Reference [12] studied the reconfiguration in resilience enhancement, but it can only restore loads in the outage area connected to the fixed tie switches. To handle these shortcomings, islanding and reconfiguration are both taken into consideration in this paper to maximize the power supply after faults.

This paper proposes an islanding and dynamic reconfiguration method to improve the resilience of distribution systems. First, the failure rate of distribution systems is generated by combining typhoon modelling and vulnerability analysis for components. The typical fault scenarios are screened according to the system information entropy. Second, an index describing the load supply level under typhoon is proposed to assess the resilience of distribution systems. A multi-stage switch strategy considering islanding and fault reconfiguration is developed based on the dynamic programming (DP). The objective is to

make a tradeoff between minimizing total power shortage and reducing the number of switching operations over the whole event's duration to obtain the optimal switch strategy. Last, the enhancement effect of islanding and dynamic reconfiguration on distribution systems resilience is analyzed.

The rest of this paper is organized as follows. In Section II, the generation of typical scenarios under typhoon is presented. Section III, a multi-stage switch strategy considering islanding and dynamic reconfiguration is presented to improve the resilience of distribution systems. Section IV demonstrates the effectiveness of the proposed method on the IEEE 33-bus distribution system. Conclusions are noted in Section V.

## II. TYPICAL FAULT SCENARIO GENERATION UNDER TYPHOON

### A. Modelling of Typhoon

When the typhoon passes, the wind speed rises sharply, making the wind loads on distribution systems components larger than their strength. Under this circumstance, the components may be damaged, leading to large-scale disconnection in the distribution systems.

The wind load is related to the wind speed and direction on the components. In this paper, the Batts model is adopted to simulate the speed and the direction of the wind during the passage of a typhoon [13]. The wind speed  $V_r$  is related to its distance  $r$  from the line to the typhoon center.

$$V_r = \begin{cases} V_{R_{\max}} r / R_{\max} & r \leq R_{\max} \\ V_{R_{\max}} (R_{\max} / r)^{0.7} & r > R_{\max} \end{cases} \quad (1)$$

where  $R_{\max}$  is the maximum wind speed radius,  $V_{R_{\max}}$  is the wind speed at this point; the wind direction at the point is the tangent direction of counterclockwise.

### B. Component Failure Rate Model under Typhoon

The failure rate model of distribution lines under the wet snow threats is established in reference [14] on the basis of a mass of statistical data. However, considering the lack of actual operating data, reference [15] builds the physical model of disturbances and calculates the failure rate of distribution lines according to the reliability theory. This kind of failure rate model of distribution lines based on the analysis of disturbance mechanism is adopted in this paper.

The force of the wire is analyzed under the influence of the wind. The total load  $N$  of the wire per unit length is the vector sum of its horizontal wind load  $N_1$  and the gravity load  $N_2$ .

$$N = \sqrt{N_1^2 + N_2^2} = \sqrt{(1.2 \times \frac{V_r^2}{1.6} D \sin^2 \theta)^2 + (qg)^2} \quad (2)$$

where  $V_r$  is the wind speed whose distance from the typhoon center is  $r$ ;  $D$  is the outer diameter of the wire.  $\theta$  is the

angle between the wind and wire;  $q$  is the mass of the wire per unit length;  $g$  is the acceleration of gravity.

Generally, the wire at the highest suspension point has the highest tension and is regarded as the most fragile. Hence, the tension of the wire at the highest suspension point is analyzed, which can be calculated as,

$$T_g^2 = T^2 + P^2 l_{gv}^2 \quad (3)$$

where  $T$  is the wire tension at the lowest point of sag;  $l_{gv}$  is the horizontal distance from the suspension point of the wire to the lowest point of the sag.

The stress  $\sigma_g$  on the section of the wire at the suspension point is,

$$\sigma_g = \frac{T_g}{S_l} \quad (4)$$

where  $S_l$  is the cross-section area of the wire.

The total load on a pole includes the horizontal load on the pole by the wire and the wind load on the pole body parallel to the wind direction. The wind load of the conductor and the wind load of the pole are

$$G_{h1} = N_1 l \quad (5)$$

$$P_p = C \frac{V_r^2}{1.6} \frac{D_0 + D_p}{2} h_p \quad (6)$$

where  $C$  is the shape coefficient;  $D_0$  and  $D_p$  are the tip diameter and root diameter of the pole;  $h_p$  is its height.

The bending moment of the pole root is the vector sum of the bending moments caused by the two wind load,

$$M = M_1 + M_2 = P_p Z + \sum_{k=1}^n P_k l h_k \quad (7)$$

where  $M_1$  is the bending moment caused by wind load on the pole body;  $M_2$  is the bending moment caused by the wind load applied by the wire on the pole;  $Z$  is the moment arm from the resultant wind pressure point of the pole to the pole root;  $P_k$  is the wind load on the  $k$ th wire;  $h_k$  is the vertical distance between the  $k$ th wire and the pole root.

As aforementioned, when the wind load on a component exceeds its strength, the component may break down. The failure rates for a wire with a stress as  $\sigma_g$  and a pole with a bending moment as  $M$  can be expressed as,

$$\begin{cases} p_l = \int_0^{\sigma_g} \frac{1}{\sqrt{2\pi}\delta_l} \exp[-\frac{1}{2}(\frac{\sigma_l - \mu_l}{\delta_l})^2] d\sigma_l \\ p_p = \int_0^M \frac{1}{\sqrt{2\pi}\delta_p} \exp[-\frac{1}{2}(\frac{M_p - \mu_p}{\delta_p})^2] dM_p \end{cases} \quad (8)$$

where  $p_l$  and  $p_p$  represent the failure rate of wire and pole;  $\sigma_l$  and  $M_p$  are the tensile strengths of the wire and the bending strength of the pole;  $\mu_l$  and  $\delta_l$  are the mean and standard deviation of the wire tensile strengths while  $\mu_p$  and  $\delta_p$  are those of the pole bending strength [16-17].

Only all the wires and poles on the line do not break down, the distribution line will operate normally, which can be described as a series model. By combining the failure rates of the wires and the poles, the failure rate  $p$  of the distribution line under the  $V_r$  can be calculated as,

$$p(V_r) = 1 - \prod_{k=1}^{n_l} (1 - p_{l,k}(V_r)) \prod_{k=1}^{n_p} (1 - p_{p,k}(V_r)) \quad (9)$$

where  $n_l$  is the span number on the distribution lines;  $n_p$  is the number of poles;  $p_{l,k}$  is the failure rate of the  $k$ th wire on the line;  $p_{p,k}$  is the failure rate of the  $k$ th pole on the line.

### C. Typical Fault Scenario Screening Based on System Information Entropy

Due to the numerous components in distribution systems, the preconceived fault scenarios are so massive that it is impossible to perform resilience analysis for all scenarios. To address this issue, typical fault scenarios need to be screened.

The concept of information entropy was first proposed to describe the degree of system disorder [18]. A distribution system can be regarded as an uncertain system, comprising lots of uncertain events where faults may occur anytime at any component. The entropy of a distribution system can be described as,

$$W = \sum_{t \in T} \sum_{i \in \Omega_B} (-\log_2 P_{i,t}) Z_{i,t} \quad (10)$$

where  $T$  represents the typhoon passage time;  $\Omega_B$  is the distribution system line set;  $Z_{i,t}$  is the operating state of the  $i$ th line at time  $t$  to describe whether the fault occurs or not.  $Z_{i,t}$  is a binary variable, and if it is 1, the  $i$ th line will encounter a fault at time  $t$ . The probability that  $Z_{i,t}$  is equal to 1 depends on  $P_{i,t}$ . The entropy of failure scenarios is calculated and the distribution of the entropy is obtained. Based on the distribution of the entropy  $W$ ,  $W_{\min}$  and  $W_{\max}$  can be obtained. If the entropy of a failure scenario is too small or too big reflecting that the probability of this scenario occurring is extremely low, this failure scenario can be considered atypical. By this means, typical fault scenarios can be screened as (11) according to the entropy of fault.

$$\begin{cases} W_{\min} \leq \sum_{t \in T} \sum_{i \in \Omega_B} (-\log_2 P_{i,t}) Z_{i,t} \leq W_{\max} \\ \sum_t Z_{i,t} \leq 1 \end{cases} \quad (11)$$

Typical fault scenarios with high probabilities of occurrence and serious consequences can be screened for further resilience analysis.

## III. ISLANDING AND RECONFIGURATION BASED ON DYNAMIC PROGRAMMING FOR RESILIENCE ENHANCEMENT

### A. Index for Resilience Assessment

When a typhoon passes, the lines in a distribution system may encounter faults, and thus the power supply gradually falls to the lowest level. Thereafter, the distribution system maintains the minimum-level power supply after the faults until the typhoon has passed. After the typhoon's passage, the operators carry out emergency repair for the damaged components. The distribution systems will gradually recover from outages and the loads will gradually rise to the normal operating level. The fault and response process of the distribution systems represented by load value is demonstrated in Fig.1.

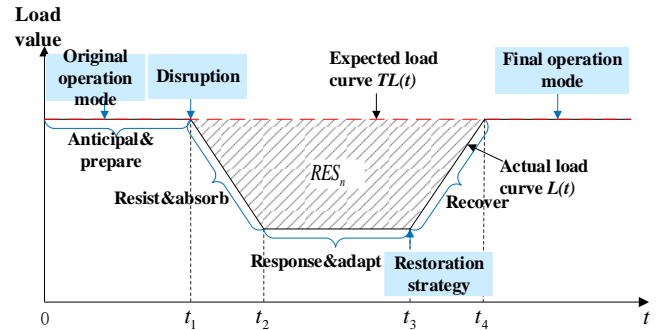


Figure 1 The fault and response process of distribution systems under typhoon

In this paper, both the duration and the severity of the faults are considered when assessing the resilience of distribution systems. The loss load caused by power outages is reflected by the loss area of the load curve under fault and that under normal conditions during the typhoon's passage. The percentage of guaranteed load supply is taken as the resilience assessment index, which is given as follows:

$$AR = \frac{\int_0^{T_0} L(t) dt}{\int_0^{T_0} TL(t) dt} = \frac{\int_0^{T_0} TL(t) dt - RES_n}{\int_0^{T_0} TL(t) dt} \quad (12)$$

where  $AR$  is the resilience assessment index under typhoon;  $T_0$  is the duration when the distribution system is affected by the typhoon, including the typhoon transit time and the power supply recovery time, that is the time span from  $t_1$  to  $t_4$  in Fig.1;  $TL(t)$  represents the expected load curve of distribution systems in normal operation;  $L(t)$  represents the actual load curve of fault operation of distribution systems under typhoon;  $RES_n$  represents the area between the expected load curve and the actual load curve in Fig.1, which is actually the power supply lost.

## B. Islanding and Reconfiguration Method for Resilience Enhancement

There are some normally-open tie switches in the distribution systems. When faults occur, tie switches and segment switches both adjust their states to change the system topology. By closing tie switches, some outage areas can be connected to the main network and thus recovered power supply through reconfiguration. By opening the segment switches, islanding can be formed to supply loads in the islands. The islanding and reconfiguration can maximize the power supply of critical loads to enhance the resilience.

At the fault time, an outage area is formed due to a fault line. The distribution systems can be reconfigured by closing tie switches connected to the outage areas. Every tie switch determines whether to close considering the balance of minimizing the load loss and reducing the cost of switch operations. Moreover, an island is formed by opening a segment switch in the proper position in the outage area during the fault time. Islanding can limit the power supply range to maximize the utilization rate of DGs, which ensures the supply of loads in islands.

However, when performing the reconfiguration, the closure of the multiple tie switches in the outage area may lead to looped networks. The distribution systems should keep radial during the reconfiguration process. Once the looped network is formed, a loop switch should be turned off to meet the radial constraints, which can be expressed as [19],

$$\sum q = N_{bus} - N_{sub} \quad (13)$$

where  $\sum q$  is the total number of closed lines;  $N_{bus}$  is the number of buses;  $N_{sub}$  is the number of the isolated islands caused by the fault lines in the system.

When the looped network has been searched for, a switch in the loop should be opened to break the loop and thus to keep the radial topology. The opening of each different segment switch in the loop will constitute a switch strategy.

The selection of the multi-stage optimal switch strategy is demonstrated in Section III.D.

## C. Optimal Load-shedding Model

Considering the capacity limitation of the gas turbine (GT), the loads in the islands cannot be fully supplied by the GT in this outage area. Moreover, the distribution lines have the limited power transmission capacities. If the power transmitted through the line exceeds the limit, the system operation security will be endangered. Therefore, considering the limitations of the above two aspects, the optimal load shedding is performed in this paper to ensure the maximum load supply. Besides, the power supply of critical loads is guaranteed in priority considering the different criticality of loads.

The objective of the optimal load shedding is to minimize the equivalent electricity loss during a typhoon passage considering the different criticality of loads.

$$\min L = \sum_{i,t} w_i \tau_{i,t} \quad (14)$$

where  $w_i$  is the importance weight of the  $i$ th load.  $\tau_{i,t}$  is the shed active loads at bus  $i$  at time  $t$ .

The constraints include power constraints on nodes, gas turbine efficiency constraints, shedding load constraints, nodal voltage constraints, gas turbine air intake constraints, and line capacity constraints:

$$\left\{ \begin{array}{l} P_{gk,t} - P_{di,t} + \tau_{i,t} - V_{i,t} \sum_{j \in i} V_{j,t} (G_{i,j} \cos \theta_{ij,t} + B_{ij} \sin \theta_{ij,t}) = 0 \\ Q_{gk,t} - Q_{di,t} + \zeta_{i,t} - V_{i,t} \sum_{j \in i} V_{j,t} (G_{ij} \sin \theta_{ij,t} - B_{ij} \cos \theta_{ij,t}) = 0 \\ P_{gk,t} = \eta_k f_{k,t} \quad \forall k \in G \\ 0 \leq \tau_{i,t} \leq P_{di,t} \\ 0 \leq \zeta_{i,t} \leq Q_{di,t} \\ V_i^{\min} \leq V_{i,t} \leq V_i^{\max} \\ f_k^{\min} \leq f_{k,t} \leq f_k^{\max} \quad \forall k \in G \\ S_i \leq S_{i \max} \end{array} \right. \quad (15)$$

where  $P_{gk,t}$  and  $Q_{gk,t}$  are the active and reactive outputs of gas turbine  $k$  at time  $t$ ;  $P_{di,t}$  and  $Q_{di,t}$  are the active and reactive power demands of bus  $i$  at time  $t$ ;  $\eta_k$  is the energy conversion efficiency of the  $k$ th gas turbine;  $G$  is the gas turbine set;  $\zeta_{i,t}$  is the reactive power shedding loads of bus  $i$  at time  $t$ ;  $V_{i,t}$  is the nodal voltage of bus  $i$  at time  $t$ ;  $f_{k,t}$  is the gas intake of gas turbine  $k$  at time  $t$ ;  $V_i^{\min}$  and  $V_i^{\max}$  are the upper and lower limits of the nodal voltage of bus  $i$ ;  $f_k^{\min}$  and  $f_k^{\max}$  are the minimum and maximum gas production of gas turbine  $k$ ;  $S_{i \max}$  is the limits of transmission power of line  $i$ .

By solving the optimization of the above model, the load shedding under different reconfiguration schemes can be obtained, and thus the load curves can be formed.

## D. The Dynamic Switch Strategy Based on Dynamic Programming Algorithm

With the development of extreme weather, the distribution lines fault successively. Hence, the switches can be adjusted at each fault time in the process of failure. It is a typical multi-stage decision-making problem, which is suitable to be solved by DP algorithm.

The multi-stage decision-making problem can be divided into several interrelated stages. For each stage, a set of

decisions that can be selected [20]. The decision of each stage is integrated to form a decision sequence, called a strategy. Obviously, there are a series of different strategies corresponding to the whole process due to the different selection decisions in each stage. What is more, the decision at the previous moment will affect the decision of the latter one. At each time step, according to the decision of the islanding and reconfiguration, the chosen tie-switches are closed and segment switches are opened for islanding to supply loads in the outage areas. Therefore, the optimal switch strategy for the whole process should be selected from the dynamic switch strategy. Dynamic switch strategy is shown in Fig.2.

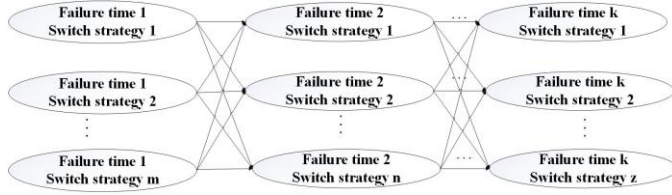


Figure 2 Dynamic switch strategy

The selection of optimal dynamic switch strategy is to make a tradeoff between minimizing the total load loss caused by the faults and reducing the cost of switch operations, considering the power supply reliability and the economy. Hence, the overall objective for the multi-stage switch strategy can be expressed as:

$$\min f = a \frac{\int_0^{T_0} TL(t) - L(t) dt}{\int_0^{T_0} TL(t) dt} + b \frac{\sum_{k=1}^N K(k)}{N} \quad (16)$$

where  $K$  is the total number of switch operations;  $N$  is the total number of switches;  $a$  and  $b$  are the weight coefficients of 2 objectives. In this paper, the main target is to supply loads in priority. Hence the weight coefficient  $a$  has the larger value.

In order to clearly indicate the resilience enhancement strategy, a flowchart is shown in Fig. 3.

#### IV. CASE STUDY

##### A. Overview of the Case

As shown in Fig.4, the proposed method has been tested on a modified IEEE 33-bus distribution system, whose data can be found in [21]. It's a 37-line radial system with total load demand of 3715kW. Five buses are modified to connect with gas turbines [22], including bus 13, 16, 20, 24, and 30. Energy conversion efficiency, output limitation, and line capacity constraint can be found in [23]. The average span of overhead distribution lines is 50m. The wire type used in this paper is LGJ-240/30, whose diameter  $D$  is 21.6mm. The diameter of the pole is 230mm, and the height is 12m. The load importance classification and corresponding weight of each load node are shown in Table I.

The coordinates are established based on the origin of bus 1 as shown in Fig. 4. It is assumed that the landing location of the typhoon is (-150km, -120km). The speed of the typhoon is

20km/h and the angle between the moving direction and the positive direction of the abscise-coordinate is  $45^\circ$ . The time of landing typhoon is 24 hours.

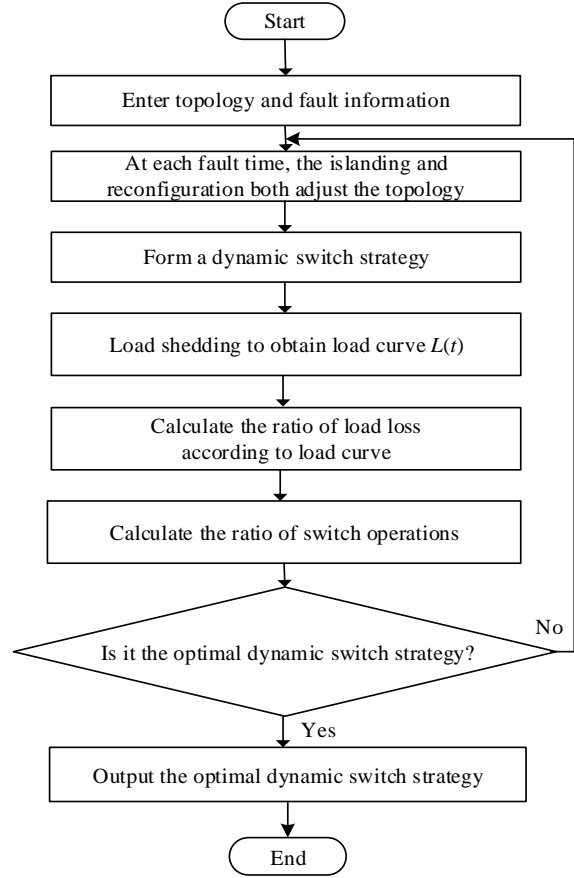


Figure 3 A flowchart to resilience enhancement strategy

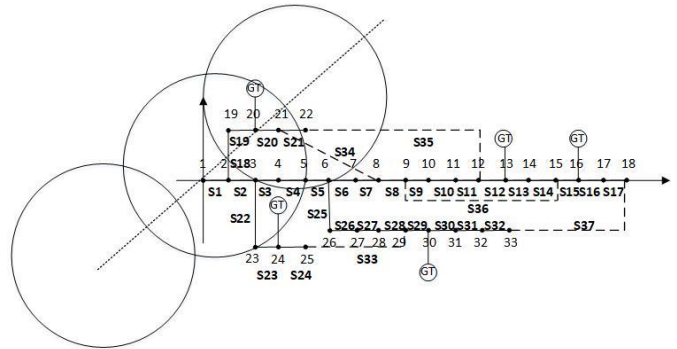


Figure 4 Diagram of the modified IEEE 33-bus distribution systems

TABLE I. LOAD PRIORITY

Load Grade	Weight	Load Bus
1	1	1, 5, 12, 15, 19, 28
2	0.1	4, 6, 8, 9, 11, 13, 16, 17 2, 3, 7, 10, 14, 18, 20, 21, 22, 23, 24, 25, 26, 27, 29,
3	0.01	30, 31, 32, 33

### B. Typical Fault Scenario Screening

The time-varying failure rate curve of line S16 is shown in Fig.5. When the typhoon passes, the line has the maximum wind speed at the maximum wind speed radius.

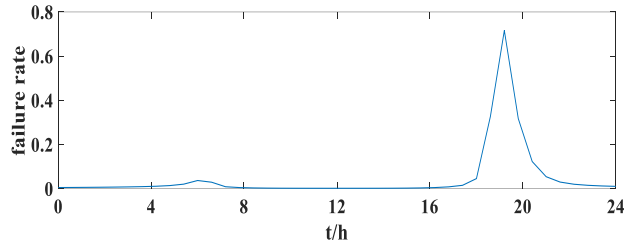


Figure 5 Time-varying fault rate curves of the line 16

Typical fault scenarios are screened with system information entropy, and the probability distribution of entropy value is shown in Fig.6.

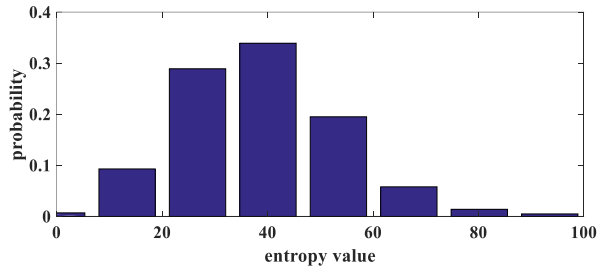


Figure 6 Entropy probability distribution

It can be seen that the system information entropy is centrally distributed in (20, 60). Thus,  $W_{min}$  and  $W_{max}$  are set to be 20 and 60 for typical fault scenario screening. The number of fault lines is statistically calculated, which is shown in Fig.7.

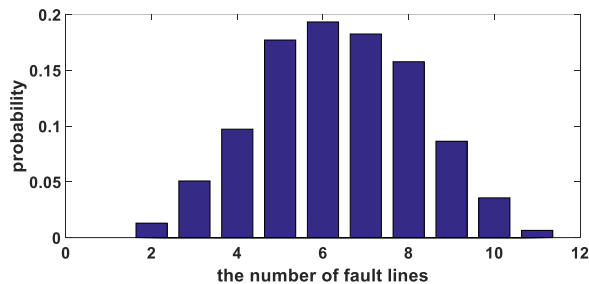


Figure 7 Probability distribution of fault lines number

It can be seen that the typical number of fault lines is 4-9. Accordingly, in the process of resilience analysis, the typical number of fault lines to be considered is mainly 4-9.

Hence, taking the 5-fold fault as an example, a typical fault scenario meeting the requirements of information entropy is selected. In this scenario, lines S30, S22, S6, S15, and S7 broke down at 7h, 7.75h, 8h, 8.25h, and 9.25h after the typhoon landed, respectively.

### C. Resilience Enhancement Based on Islanding and Reconfiguration

The resilience is assessed during the whole typhoon passage. In this scenario, the multi-stage switch strategy based on dynamic programming is displayed in Table II.

t/h	Fault Lines	Switch Strategy
7.00	S31	S37 close
7.75	S22	S24 open
8.00	S6	S7 open
8.25	S15	S31 open S12 open
9.25	S7	S35 close
		-

Based on the switch strategy, the load curves for normal operation and for the fault scenario with and without resilience enhancement by load shedding model are demonstrated in Fig.8 and the result for resilience assessment is displayed in Table. III.

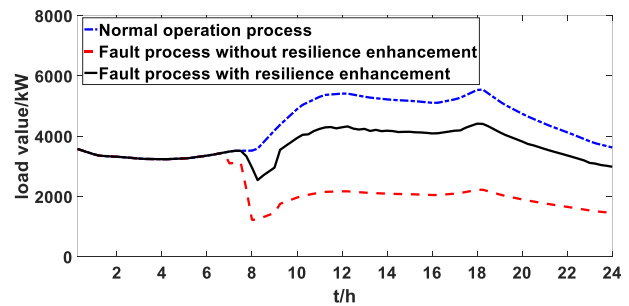


Figure 8 Load curves of distribution systems in different situations

TABLE III. ASSESSMENT OF DISTRIBUTION SYSTEMS RESILIENCE

	Without Resilience Enhancement	With Resilience Enhancement
Load Loss/MWh	310	223
Index AR Resilience	0.3245	0.8478
Enhancement Ratio	-	52.33%

It can be seen that, without considering resilience enhancement, the assessment index AR of distribution systems resilience is 0.3245, which means only 32.45% of the electricity demand can be supplied. After enhancing the resilience based on the proposed resilience enhancement method, the assessment index AR increases to 0.8478. In other words, 84.78% of the power supply can be ensured. The resilience of the distribution system is improved significantly by 52.33%. Hence the distribution system resilience can be enhanced effectively through the proposed islanding and dynamic reconfiguration.

## V. CONCLUSION

Taking typhoon as the representative of extreme weather, this paper proposes a resilience enhancement method considering islanding and dynamic reconfiguration. When faults occur, the islanding and reconfiguration both adjust the topology to reduce the load loss. Based on the dynamic programming, a multi-stage switch strategy is proposed. The switch strategy is adjusted in time with the fault process of successive disconnection of the distribution systems under extreme weather. The optimal dynamic switch strategy can make a tradeoff between minimizing the total power shortage and reducing the cost of switch operations. Simulation results prove the effectiveness of the method proposed in this paper. The load loss in the process of extreme weather can be reduced and the power supply can be ensured to the most extent. The resilience of distribution systems can be enhanced effectively.

## ACKNOWLEDGMENT

This work was supported by the Science and Technology Project of State Grid Corporation of China (52060019001H).

## REFERENCES

- [1] G. Li et al., "Risk analysis for distribution systems in the northeast U.S. under wind storms," *IEEE Trans. Power Syst.*, vol. 29, no. 2, pp. 889-898, Mar. 2014.
- [2] N. Onizawa, A. Mochizuki, A. Tamakoshi, and T. Hanyu, "A sudden power-outage resilient nonvolatile microprocessor for immediate system recovery," in *Proc. IEEE/ACM Int. Symp. Nanoscale Architectures*, vol. 15, pp. 39-44, Sep. 2016.
- [3] P. Hines, J. Apt, and S. Talukdar, "Large blackouts in North America: Historical trends and policy implications," *Energy Pol.*, vol. 37, pp. 5249-5259, Jan. 2009.
- [4] D. M. Ward, "The effect of weather on grid systems and the reliability of electricity supply," *Climatic Change*, vol. 121, pp. 103-113, Sep. 2013.
- [5] Y. Y. Haimes, "On the definition of resilience in systems," *Risk Anal.*, vol. 29, pp. 498-501, Apr. 2009.
- [6] R. Francies and B. Bekera, "A metric and frameworks for resilience analysis of engineered and infrastructure systems," *Reliab. Eng. Syst. Saf.*, vol. 121, pp. 90-103, Jul. 2013.
- [7] J. H. Kahan, A. C. Allen, and J. K. George, "An operational framework for Resilience," *J. Homeland Secur. Emergency Manage.*, vol. 6, pp. 1-48, Dec. 2009.
- [8] D. Henry and J. E. Ramirez-Marquez, "Generic metrics and quantitative approaches for system resilience as a function of time," *Reliab. Eng. Syst. Saf.*, vol. 99, pp. 114-122, Oct. 2012.
- [9] M. Panteli, P. Mancarell, S. Wilkinson, and R. Dawson, "Assessment of the resilience of transmission networks to extreme wind events", in *Proc. IEEE Eindhoven PowerTech*, Jun/Jul. 2015, pp. 1-6.
- [10] A. M. Salman, Y. Li, and M. G. Stewart, "Evaluating system reliability and targeted hardening strategies of power distribution systems subjected to hurricanes," *Reliab. Eng. Syst. Saf.*, vol. 144, pp. 319-333, Jul. 2015.
- [11] C. Chen, J. Wang, F. Qiu, and D. Zhao, "Resilient distribution system by microgrids formation after natural disasters," *IEEE Trans. Smart Grid*, vol. 7, pp. 958-966, Jun. 2015.
- [12] G. Vaskantiras and Y. Shi, "Value assessment of distribution network reconfiguration: a Danish case study," *Energy Procedia*, vol. 100, pp. 336-341, Oct. 2016.
- [13] M. E. Batts, E. Simiu, and L. R. Russell, "Hurricane wind speeds in the United States," *J. Struct. Div.*, vol.106, pp. 2001-2016, May. 1980.
- [14] S. Ge, J. Li, L. Hong, Y. Cao, Z. Yang, and J. Yun, "Assessing and boosting resilience of distribution system under extreme weather," *IEEE PES General Meeting*, Atlanta, pp. 1-5, Aug. 2019.
- [15] E. Ciapessoni, D. Cirio, A. Pitto, and M. Sforna, "A probabilistic risk-based security assessment tool allowing contingency forecasting," *PMAPS 2018 Conf.*, Boise, pp. 1-6, June. 2018.
- [16] T. Gonen, "Electrical power transmission system engineering analysis and design," 2nd ed. Boca Raton, FL, USA: CRC, 2009.
- [17] L. L. Grigsby, "The electrical power engineering handbook: electrical power generation, transmission and distribution," New York: CRC/IEEE, 2001.
- [18] C. E. Shannon and W. W. Weaver. *A Mathematical Theory of Communications*. Urbana, IL; Univ. of Illinois Press, 1949.
- [19] Y. Lin and Z. Bie, "Tri-level optimal hardening plan for a resilient distribution system considering reconfiguration and DG islanding," *Appl. Energy*, vol. 210, pp. 1266-1279, Jun. 2018.
- [20] M. H. Shariatkhah, M. R. Haghifam, J. Salehi, and A. Moser, "Duration based reconfiguration of electric distribution networks using dynamic programming and harmony search algorithm," *Int. J. Elec. Power Energy Syst.*, vol. 41, pp. 1-10, Dec. 2012.
- [21] S. Ghasemi and J. Moshtagh, "Radial distribution systems reconfiguration considering power losses cost and damage cost due to power supply interruption of consumers," *Int. J. Elect. Eng. Inform.*, vol. 5, pp. 297-315, Sep. 2013.
- [22] Y. Du, T. Zhang, and W. Zhang, "Enhancing distribution system resilience to extreme weather using multi-energy coordination," in *Proc. IEEE PES Asia-Pacific Power Energy Eng. Conf. (APPEEC)*, Macao, pp. 1-5, Dec. 2019.
- [23] S. Qi, X. Wang, C. Shao, Y. Bian, Y. Wang, and L. Yao, "Resilience analysis of integrated electricity and natural gas energy system under extreme events," *Power Syst. Technol.*, vol. 43, pp. 41-51, Jan. 2019. (in Chinese)